Absolute Measurements of the 2^1P and 2^3P Electron Excitation Cross Sections of Helium Atoms*

JOHN D. JOBE AND ROBERT M. ST. JOHN
Department of Physics, University of Oklahoma, Norman, Oklahoma
(Received 9 June 1967)

The apparent cross sections for electron excitation of the 2^1P and 2^3P states of helium are examined in the light of new and detailed information concerning the cascading to these levels from higher states, particularly in the low-energy region near onset. Excitation functions of the ^1S, ^1D, ^3S, and ^3D states from $n=3$ to $n=7$ or 8 are presented in this energy range. Absolute measurements of the apparent cross sections of 22 of these states are also given. Excitation functions for the $2P$ states are presented for low-energy and extended-energy ranges. After allowance is made for imprisonment in the 2^1P state, the cascading corrections yield the cross sections for direct electron excitation to the 2^1P and 2^3P states over the energy range from onset to 450 eV. The maximum value for the 2^1P state is 9.2×10^{-18} cm^2, and for the 2^3P state is 2.2×10^{-18} cm^2. The results show good agreement with theoretical calculations for energies greater than 100 eV, but poor agreement in the low-energy range.

I. INTRODUCTION

Up to the present time, no absolute cross section values for the lowest-lying P states of helium have been available. This is mainly due to the fact that the transitions from these states lie in spectral regions where standard detection techniques are rather insensitive. This paper is concerned with the experimental methods and subsequent analysis of data that lead to absolute values for the electron excitation cross sections of the 2^1P and 2^3P states.

Section II deals briefly with the experimental method and data processing system. Since cascading from higher states is an important process in the population of the $2P$ states we present in Sec. III the results of a detailed investigation concerning these states. In Sec. IV these and other results are used in order to correct the apparent cross sections of the $2P$ states. Finally, in Sec. V we discuss the results in the light of theory.

II. EXPERIMENTAL METHOD

The apparatus used for measuring the excitation functions is shown in Fig. 1. The essential features for automatically processing the date and recording the relative excitation functions are the same as those described in a previous paper.[1] A signal which is proportional to the relative cross section plus noise is obtained at the output of an analog divider and fed to the recording device along with the electron accelerating voltage. A recent addition (not shown in Fig. 1) to this system is an automatic excitation function averaging device. This device, a Nuclear Data Model ND-800 Enhancetron, samples the divider output at 1024 equally spaced increments during the accelerating voltage sweep and stores this information in its memory unit. On each successive voltage sweep the corresponding divider outputs are added to those previously stored and in this manner random noise is significantly reduced.

The purpose of the detection system is to measure the photon emission rate at a particular wavelength from the excitation region. For the 2^1P and 2^3P states these wavelengths are 20 582 and 10 832 Å, respectively. In order to measure this radiation a Kodak Ektron type-N lead sulfide detector was used. The dimensions of the sensitive area were 0.1×1.0 cm. This detector has a time constant of approximately 500 μsec and was operated at 25°C. Because of the relative insensitivity of lead sulfide detectors in comparison with photomultiplier tubes, high source intensity becomes of prime importance. For this reason a rather large electron gun producing a 1-cm-diam beam was employed. This electron gun is an electrostatically focused pentode type with a dispenser cathode. Beam currents normally used are 2 to 10×10^{-3} A. The gun is located in a stainless-steel high-vacuum chamber equipped with sapphire windows.

Absolute measurements are obtained in the usual manner by calibration against a tungsten ribbon

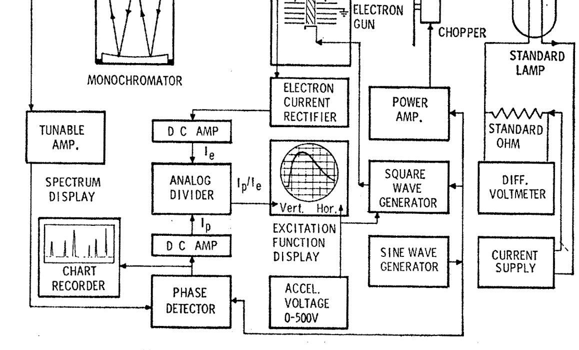

FIG. 1. Arrangement of the experimental apparatus.

---

* Research sponsored by the U. S. Air Force Office of Scientific Research, Office of Aerospace Research, U. S. Air Force, under AFOSR Grant No. 252-67.

[1] R. M. St. John, C. C. Lin, R. L. Stanton, H. D. West, J. P. Sweeney, and E. A. Rinehart, Rev. Sci. Instr. 33, 1089 (1962).

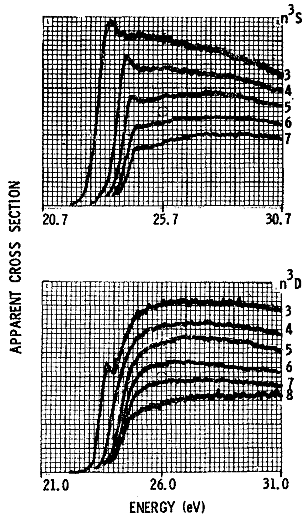

FIG. 2. Apparent cross sections of states cascading to the 2^3P level at 5 μ pressure. The vertical scale for each curve is fixed by its value at 27 eV given in Table I. The 5^3D contains contributions from the 7^1S.

standard lamp. The method differs from that given in Ref. 1 in several ways. As shown in Fig. 1, the standard lamp is in direct line with the collision chamber window and monochromator. Also, the light from the standard lamp is chopped mechanically and in phase with the electronically chopped beam; hence, standarization of a line may be made simultaneously with or immediately following its observation with no rearrangement of the optical system. Emissivity values for tungsten in the infrared were obtained from the work of DeVos.[2]

Wavelength selection was achieved through the use of interference filters or monochromators of $\frac{1}{4}$- and $\frac{1}{2}$-m focal length equipped with gratings of 0.3-, 0.6-, 1.2-, and 2.1-μ blaze.

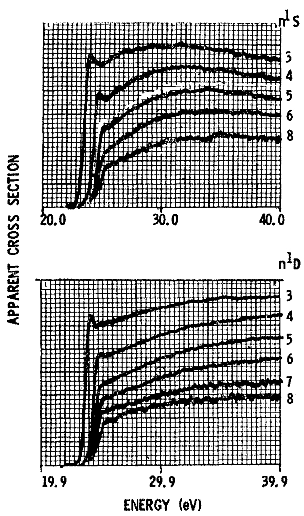

FIG. 3. Apparent cross sections of the states cascading to the 2^1P level at 5-μ pressure.

[2] J. C. DeVos, Physica **20**, 690 (1954).

III. THE CASCADING STATES

Existing information concerning the apparent cross sections of those states that cascade to the 2^1P and 2^3P levels was not complete enough to allow a detailed cascade analysis of these levels near threshold. For this reason, absolute apparent cross sections for 22 of these states were measured at 27-V energy and a pressure of 5 μ. These values are presented in Table I. The excitation functions are shown in in Figs. 2 and 3. Smit, Heideman, and Smit[3] have reported near threshold excitation functions for 11 of these levels. The shape agreement is good if one allows for their slightly better energy resolution. It is estimated from the curves reported herein that the half-width energy spread of our electron beam at 5 μ is in the 0.4- to 0.5-eV range. This is quite good since the beam currents used for this data were 2 to 5×10^{-3} A.

TABLE I. Apparent cross sections of the 2P states and some of their cascading states at 5 μ pressure. The 2^1P value is corrected for imprisonment. The lines marked * are unresolved. The 7^1S value is interpolated (from the 6, 8^1S) and used as a correction on the total transition to obtain the 5^3D value.

Transition observed (Å)	State	Apparent cross section (10^{-20} cm²) 27 eV	Maximum
20582	2^1P	286	1020
10832	2^3P	400	400
7281	3^1S	56	58
7065	3^3S	95	107
6678	3^1D	32	36
5876	3^3D	32	32
5048	4^1S	20	23
4922	4^1D	14	19
4713	4^3S	32	35
4471	4^3D	14	14
4438	5^1S	9.4	11
4387	5^1D	7.6	11
4169	6^1S	5.0	6.3
4144	6^1D	4.2	5.9
4121	5^3S	15	16
*4026	5^3D	7.5	7.5
*4025	7^1S	2.9	3.8
4009	7^1D	2.2	3.1
3937	8^1S	1.8	2.5
3926	8^1D	1.6	2.2
3867	6^3S	8.5	8.5
3820	6^3D	5.0	5.0
3733	7^3S	5.0	5.2
3705	7^3D	3.3	3.3
3634	8^3D	2.1	2.2

Oscillograms of each family of cascading states were obtained by a multiple exposure technique, the monochromator being adjusted to the proper wavelength between exposures. The energy scale for each family is measured relative to the 2^3P onset, which was taken at its spectroscopic value of 21.0 V. When this is done, all

[3] C. Smit, H. G. M. Heideman, and J. A. Smit, Physica **29**, 245 (1963).

other onsets appear very nearly at their corresponding spectroscopic values.

IV. ANALYSIS OF DATA

A. The 2^3P State

The equation relating the steady-state population gain and loss rates per unit volume for the 2^3P state can be written as

$$\underbrace{Q(2^3P)\frac{IN}{eS}}_{\text{direct electron excitation}}+\underbrace{\sum_{n=3}^{\infty}[N(n^3S)A(n^3S-2^3P)+N(n^3D)A(n^3D-2^3P)]}_{\text{cascade}}=\underbrace{N(2^3P)A(2^3P-2^3S)}_{\text{radiative loss}}. \quad (1)$$

Here N and $N(n^3k)$ represent the ground-state and excited-state densities, respectively. I/e is the rate at which electrons pass through the gas in a beam of cross-sectional area S. $Q(2^3P)$ is the cross section for direct electron excitation and the A's are transition probabilities. The values of the transition probabilities used are the ones tabulated by Gabriel and Heddle.[4]

The quantity which is directly related to the experimental measurements is the apparent cross section for excitation to the kth state, defined as

$$Q'(k)=(eS/IN)N(k)A(k), \quad (2)$$

where $A(k)$ represents the total transition probability from this state. When the observed transition kj is only one of several, we introduce the branching ratio

$$B(kj)=A(k)/A(kj) \quad (3)$$

so that

$$Q'(k)=(eS/IN)N(k)B(kj)A(kj). \quad (4)$$

The steady-state equation can now be written

$$Q(2^3P)=Q'(2^3P)-\sum_{n=3}^{\infty}\left[\frac{Q'(n^3S)}{B(n^3S-2^3P)}+\frac{Q'(n^3D)}{B(n^3D-2^3P)}\right], \quad (5)$$

or simply

$$Q(2^3P)=Q'(2^3P)-Q_c(2^3P), \quad (6)$$

where the last term represents the cascading summation.

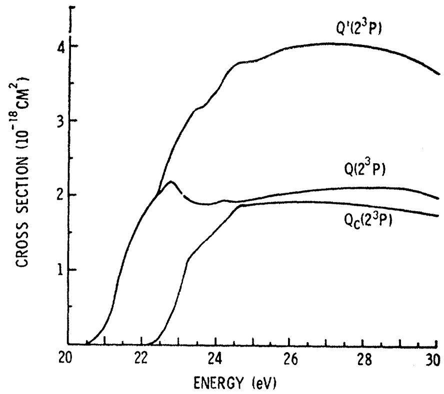

FIG. 5. Cascading correction to the 2^3P level at low energy. $Q'(2^3P)$ is the apparent cross section, $Q_c(2^3P)$ is the cascade to the 2^3P level, and $Q(2^3P)$ is the corrected cross section.

The apparent cross section of the 2^3P state for two energy ranges is shown in Fig. 4. For the 20- to 30-V range, the cascade contribution was calculated from the data discussed in Sec. III. For the unmeasured cascading states ($n>7$ or 8), the small contribution to Q_c ($<7\%$) was determined by extrapolation from the n^{-x} law where x was determined from the data of the lower states. The unmeasured excitation-function shapes for high n were assumed to be similar to that of the highest state measured. Q', Q_c, and Q for the 2^3P state are shown in Fig. 5.

In the higher-energy range the shapes of the apparent cross sections of the cascading states are similar and the corresponding corrections to $Q'(2^3P)$ are simplified. The corrected cross section over the entire energy range investigated is shown in Fig. 6.

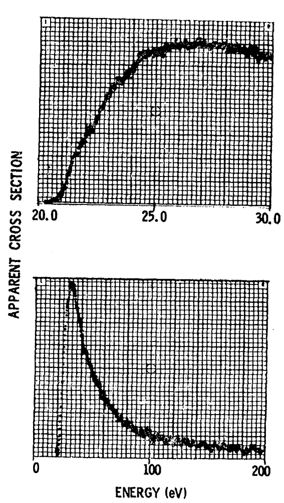

FIG. 4. Apparent cross sections of the 2^3P state at 5 μ pressure. Both represent averages of nine separate scans. At 27 eV, $Q'(2^3P)=4.0\times10^{-18}$ cm^2.

B. The 2^1P State

Here we must consider the imprisonment of resonance radiation. If we denote by g the fraction of resonance photons that are not absorbed by the gas but escape to the absorbing walls of the collision chamber, then

[4] A. H. Gabriel and D. W. O. Heddle, Proc. Roy. Soc. (London) **A258**, 124 (1960).

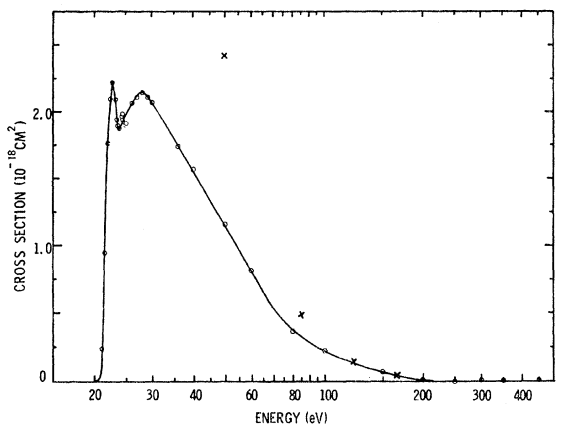

FIG. 6. The 2^3P corrected cross section. The X's are from the calculations of Massey and Moiseiwitsch (Ref. 9).

the population equation for the 2^1P states takes the form

$$\underset{\text{gain from electron excitation + cascade}}{[Q(2^1P)+Q_c(2^1P)]\frac{IN}{eS}}+\underset{\text{regained by imprisonment}}{(1-g)N(2^1P)A(2^1P-1^1S)}$$

$$=N(2^1P)\underset{\text{radiative loss}}{[A(2^1P-1^1S)+A(2^1P-2^1S)]}. \quad (7)$$

Using the definition of apparent cross section and solving for the quantity of interest, we find

$$Q(2^1P)=\frac{Q'(2^1P)}{B(2^1P-2^1S)}\times\left[g\frac{A(2^1P-1^1S)}{A(2^1P-2^1S)}+1\right]-Q_c(2^1P). \quad (8)$$

Limits on the values of g have been obtained by Phelps[5] for a collision chamber of cylindrical symmetry and radius R. From these values one may obtain g as a function of R and the pressure p for a line subject to Doppler broadening only. Gabriel and Heddle[4] have applied the analysis of Ref. 5 in order to obtain the electron excitation cross section of the 3^1P state. We use a similar analysis on the 2^1P state since we cannot detect the infrared radiation from this state at pressures low enough to give zero imprisonment. Indeed, even at 1-μ pressure, imprisonment is still about 93%.

In practice the collision chamber is usually nearly enclosed at both ends, contains viewing slots, etc., so that one no longer has ideal cylindrical geometry. One must therefore attempt to determine an effective radius ρ. One substitutes data for different values of p and ρ in the (right-hand side r.h.s.) of Eq. (8) to see if there is a unique value for $Q(2^1P)$ at all pressures. The values of $Q'(2^1P)/B(2^1P-2^1S)$ and $Q_c(2^1P)$ are obtained for various pressures from the experimental curves shown in Fig. 7. The quantity $g(\rho,p)$ is evaluated over a range

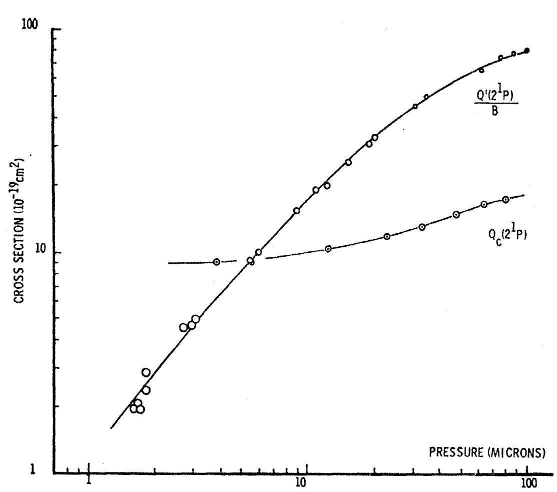

FIG. 7. Pressure dependence of the quantities $Q'(2^1P)$ and $Q_c(2^1P)$ at 100 eV.

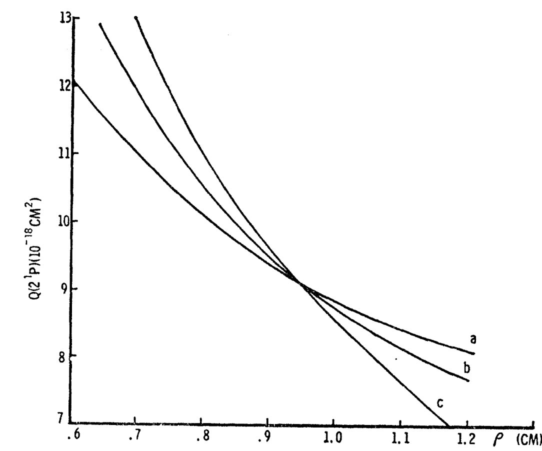

FIG. 8. Values of the right-hand side of Eq. (7) for pressures of (a) 60, (b) 30, (c) 4.5 μ.

of values of ρ for each pressure with the aid of the graph presented in Ref. 4. The results of this analysis for 100-V electrons are shown in Fig. 8. Here we have plots of $Q(2^1P)$ versus ρ for the three pressures of (a) 60, (b) 30, and (c) 4.5 μ. We see that for an effective radius of about 0.95 cm we have the solution $Q(2^1P)=9.2\times10^{-18}$ cm^2. Curves at higher pressures tended to yield lower values of $Q(2^1P)$ but at these pressures effects other than Doppler broadening become important as discussed in Ref. 5.

The cross-sectional segment of the collision area under observation was 0.5 mm in thickness and situated 0.4 cm from the end plate of the collision chamber. The end plate had a 1-cm-diam opening for admittance of the electron beam. The actual radius of the collision chamber was 1.5 cm but due to the presence of the end

[5] A. V. Phelps, Phys. Rev. **110**, 1362 (1958).

plate one would expect the effective radius to lie between 0.4 and 1.5 cm. Hence the value of the effective radius obtained from Eq. (8) lies within the limits imposed by the geometry of the collision chamber.

The cascade contribution to the 2^1P state at 100 eV shows pressure dependence due to the enhancement of the ^1D series population at high pressures by the multistate transfer process.[6] The ^1S series shows little or no pressure dependence. The shape of the excitation function of the 2^1P state, shown in Fig. 9, is typical for the ^1P states and shows only slight pressure dependence. Cascade corrections were applied at all energies in the manner described in Sec. IV A. The corrected excitation function is shown in Fig. 10.

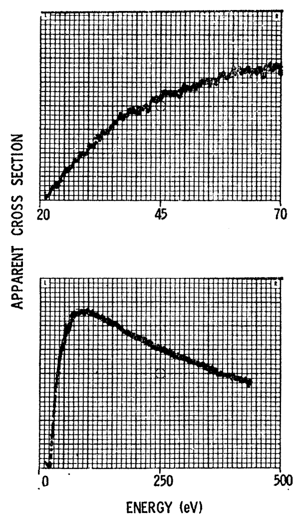

FIG. 9. Apparent cross sections of the 2^1P state. Top: average of 25 scans at 4 μ pressure. Bottom: average of 9 scans at 8 μ pressure.

The apparent cross sections of the ^1D series are significantly affected by polarization (up to 12%) and hence were corrected for this effect according to the method outlined in Ref. 7. It was not possible to determine exact polarization values for the 2^3P and 2^1P radiation at low pressure due to weak signals. However by using a Nicol prism, it was determined that the polarization was no more than 10% from onset to 100 eV at 10 μ pressure. The polarization correction for the ^3D series has a maximum value of only 4% and hence

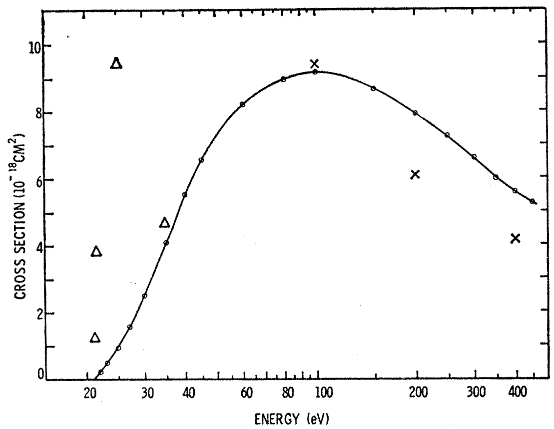

FIG. 10. Corrected cross sections for the 2^1P state. $\times$, theoretical values of Massey and Mohr (Ref. 10); $\triangle$, theoretical values of Vainshtein and Dolgov (Ref. 11).

was neglected. The polarization data of McFarland and Soltysik[8] was used.

V. DISCUSSION OF RESULTS

The cross section for the 2^3P state is noticeable for the fact that it approaches zero rapidly at energies beyond 100 eV in complete agreement with the theoretical values. Beyond 200 eV all the apparent cross section can be accounted for by cascade. The exchange distorted wave calculation of Massey and Moiseiwitsch[9] gives for the maximum of the cross section a value about 6 times our result while their Born-Oppenheimer approximation is about 13 times our result. Also striking is the sharp peak near threshold, similar to the peaks observed for the S and D states with low-n values.

The result for the 2^1P state is subject to more error than the 2^3P state due to the uncertainty in the correction for imprisonment effects. Hence we consider the agreement with the Born approximation[10] at the higher energies to be quite good. The theoretical results[11] shown for the low-energy range however predict more of a triplet-shaped function and consequently show poor agreement with our result.

ACKNOWLEDGMENTS

The authors are grateful to Paul N. Stanton and James D. Walker for their assistance in electronic design and construction.

[6] R. M. St. John and R. G. Fowler, Phys. Rev. **122**, 1813 (1961); C. C. Lin and R. G. Fowler, Ann. Phys. (N. Y.) **15**, 461 (1961); R. M. St. John and T. W. Nee, J. Opt. Soc. Am. **55**, 426 (1965).

[7] R. M. St. John, F. L. Miller, and C. C. Lin, Phys. Rev. **134**, A888 (1964).

[8] R. H. McFarland and E. A. Soltysik, Phys. Rev. **127**, 2090 (1962); **128**, 147 (1960).

[9] H. S. W. Massey and B. L. Moiseiwitsch, Proc. Roy. Soc. (London) **A258**, 147 (1960).

[10] H. S. W. Massey and C. B. O. Mohr, Proc. Roy. Soc. (London) **A140**, 613 (1932).

[11] L. A. Vainshtein and G. G. Dolgov, Opt. i Spektroskopiya [English transl.: Opt. Spectry. (USSR) **7**, 1 (1959)].